Atmospheric Research 131 (2013) 22–33

Contents lists available at SciVerse ScienceDirect

Atmospheric Research

journal homepage: www.elsevier.com/locate/atmos

Orographic low-level clouds of Southeast Asia during the cold surges of the winter monsoon

Hiroshi G. Takahashi *

Graduate School of Urban Environmental Sciences, Tokyo Metropolitan University (TMU), Tokyo, Japan
Research Institute for Global Change, Japan Agency for Marine-Earth Science and Technology (JAMSTEC), Yokohama, Japan

ARTICLE INFO

Article history:
Received 29 March 2012
Received in revised form 5 July 2012
Accepted 6 July 2012

Keywords:
Low cloud
Precipitation
Cold surge
Seasonal march of cloud and precipitation activities

ABSTRACT

This study is an examination of low clouds over Southeast Asia during northern fall and winter using albedo values derived from visible images, cloud-top temperatures from infrared radiation images from the Multi-functional Transport Satellite 1 (MTSAT-1), and rainfall-top height (storm height) from precipitation radar (PR) on the Tropical Rainfall Measuring Mission (TRMM) satellites. To understand the cloud and precipitation activities associated with the winter monsoon cold surges along the eastern coast of the Indochina Peninsula, atmospheric circulation data from the Japanese 25-year reanalysis (JRA-25) were used.

The results showed that low clouds were frequently observed in December, January, and February. In October and November, rainfall activity was relatively high, whereas, in northern winter, it was low, although the winter monsoon northeasterly was strong in both cases. The cloud-top height and storm height decreased with the seasonal march from northern fall to winter.

Also examined in this study were the temporal variations in cloud activity on shorter time scales than those of the seasonal march. Concurrent with the cold surges along the eastern coast of the Eurasia, clouds varied on synoptic and intraseasonal time scales. The timing of low-cloud formation corresponded to the beginning of the cold surges. However, the low clouds along the eastern coast of the Indochina Peninsula may remain during the weakening phase of the cold surges.

1. Introduction

Low clouds affect global climate as a result of changes in the radiation balance that mainly reduce the incoming solar energy. On Earth, distinct low clouds appear over the subtropical, mid-latitude, and Arctic oceans and the eastern coast of Eurasia (Klein and Hartmann, 1993, specifically, southern China and eastern Indochina). Distinct low clouds over land appear only over the Asian monsoon region. Klein and Hartmann (1993) also found that the low clouds of the Asian monsoon tend to appear in northern winter, which corresponds to the Asian winter monsoon season. Here, we focus on the low clouds of the Asian winter monsoon and the related precipitation activity. Chang et al. (2005b) found that the low-level northeasterly of the winter monsoon along the eastern coast of Eurasia, which originates from the Siberian High, prevails during northern fall and winter. Thus, it is possible that low clouds over the eastern coast of Eurasia are affected by the northeasterly of the winter monsoon.

Over the tropical Asian monsoon region, the eastern sides of the Indochina Peninsula, the Malay Peninsula, the Philippines, and the maritime continent are well-known as winter monsoon regions where cloud-precipitation activity is more vigorous in northern winter than in summer. The cloud-precipitation activity of the Asian winter monsoon is generally examined over the maritime continent (e.g., Houze et al., 1981; Goldenberg et al., 1990; Chang et al., 2005a; Ichikawa and Yasunari, 2006). Low clouds have been examined over the Indian Ocean (Bony et al., 2000). Chang et al. (2005b) showed that the rainfall amount over the Indochina Peninsula is larger in northern fall than in northern winter. However, the climatological monsoon northeasterly prevails throughout northern fall and winter.

* Corresponding author at: Graduate School of Urban Environmental Sciences, Tokyo Metropolitan University (TMU), Tokyo, Japan.
E-mail address: hiroshi3@tmu.ac.jp.

0169-8095/$ – see front matter © 2012 Elsevier B.V. All rights reserved.
doi:10.1016/j.atmosres.2012.07.005

They hypothesized that the seasonal difference in precipitation may be partly explained by the seasonal march of sea-surface temperature (SST) over the South China Sea. It is noteworthy that the rainfall amount in Vietnam (the eastern coast of the Indochina Peninsula) is very small during northern winter, although the northeasterly winds are strong (Matsumoto 2009: personal communication). Takahashi and Yasunari (2006, 2008) and Takahashi (2011) have indicated that tropical cyclone activity is a major contributor to the total rainfall amount in northern fall over and around the Indochina Peninsula. This may be a key factor for understanding the seasonal difference in precipitation.

Additionally, cold surges are also a typical phenomenon in the East and Southeast Asian monsoon regions during northern winter. The cold breaks bring local temperature drops in many regions and heavy precipitation, including snowfall, over the Sea of Japan side of the Japanese archipelago and strong northeasterlies over the eastern coasts of the Indochina Peninsula and the Philippines. Concurrent with the cold surges, rainfall sometimes develops over Southeast Asia (Chang et al., 2003; Yokoi and Matsumoto, 2008; Takahashi et al., 2011). Hence, it is plausible that the cold surges are one of the essential factors in the development of low clouds in the Asian winter monsoon.

Over the tropical Asian monsoon region, although cloud-precipitation activity has been investigated in boreal summer, few previous studies have examined cloud-precipitation activity in boreal winter except over the maritime continent. Furthermore, knowledge of cloud activity on shorter time scales is basically lacking, although it should help us to understand the monthly mean cloud-coverage and -formation mechanisms. In addition, in most previous studies, convective or rainfall activity was investigated exclusively, even though clouds and precipitation are closely associated. The examination of both cloud and precipitation increases the understanding of the entire system. Hence, the purpose of this study was to investigate the cloud-precipitation activity of the winter monsoon over the eastern coast of Southeast Asia. In this study, we focused specifically on cloud activity on shorter time scales, which are characteristic of mid-latitude cold surges. In this study, we also investigated the seasonal differences in cloud-precipitation characteristics within the winter monsoon period. Section 2 is a description of the data and methods used, and the cloud and precipitation climatology is presented in Section 3. In Section 4, synoptic and intraseasonal cloud activity is discussed, and, in Section 5, the conclusion is presented.

2. Data and methods

2.1. Cloud data

To understand cloud and precipitation activities, several datasets were used in this study. Cloud characteristics were examined using visible (0.55–0.90 μm, VIS)- and infrared (10.3–11.3 μm, IR1)-radiation-channel images from the Multi-

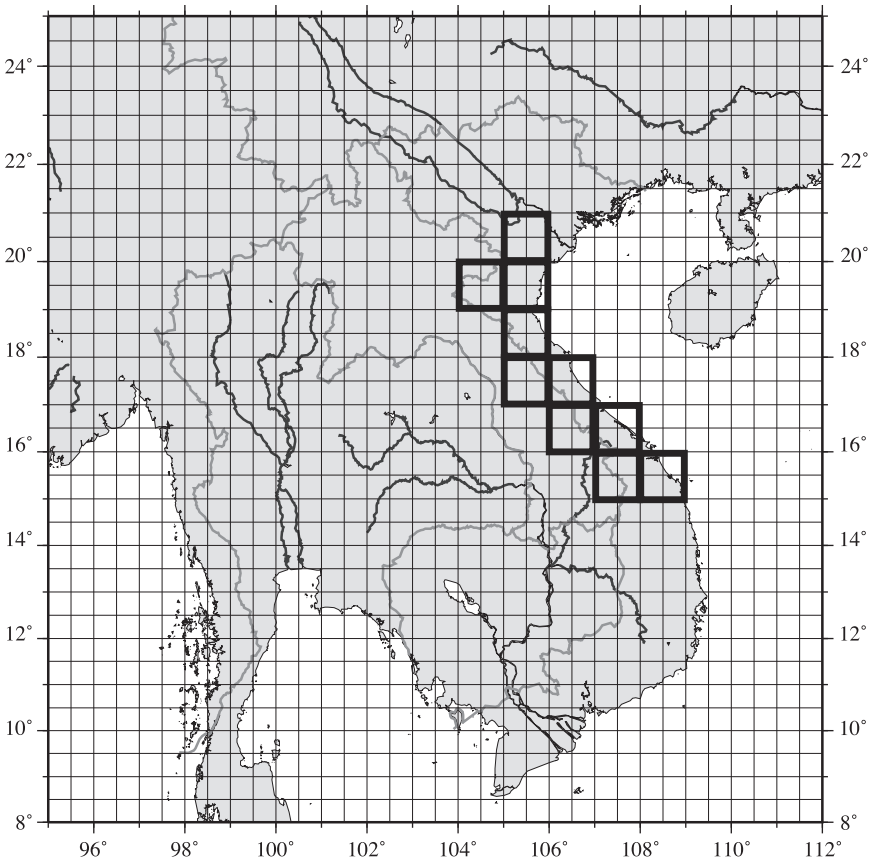

Fig. 1. Study area. Thick rectangles over the eastern coast of the Indochina Peninsula show the reference area for calculating cloud cover and cloud-top temperature.

functional Transport Satellite 1 (MTSAT-1), a Japanese geostationary satellite, which were provided by the Center for Environmental Remote Sensing (CEReS) of Chiba University, Japan. VIS-channel images were used to calculate cloud coverage, and IR1 data were used to analyze the cloud coverage and cloud-top temperature. The grid intervals of VIS and IR1 images were 0.01° and 0.04° in longitude and latitude, respectively. Unphysical counted values are provided for both VIS and IR1. To convert physical values, such as albedos and brightness temperature, calibration tables were also provided for VIS and IR1. Gridded data were used in this study. The VIS images at 04:30 UTC (11:30 local solar time (LST) along 105°E) were used. Hourly IR1 images were also used. To understand the climatology of cloud and precipitation activities, 4-year data from October 2006 to March 2010 were used. To discuss cloud cover over the eastern Indochina Peninsula, this study defined the reference area shown in Fig. 1. The area is based on the monthly mean cloud frequency, which is shown in Fig. 4.

2.2. Rainfall data

To understand the temporal–spatial characteristics of precipitation activity over the Southeast Asian monsoon region, this study used the Tropical Rainfall Measuring Mission Precipitation Radar (TRMM-PR, Iguchi et al., 2000), Global Satellite Mapping of Precipitation Microwave Radiometer (GSMaP-MWR, Kubota et al., 2007), and TRMM3B42 (Huffman et al., 2007) datasets. Because few previous comparisons have been made of different rainfall datasets for this region during the winter monsoon, the characteristics and biases of rainfall data have not yet been revealed. Because the rainfall amounts from different datasets deviate strongly in the current situation, cross-checks among the rainfall datasets are required.

The spatial resolution of TRMM-PR, GSMaP-MWR, and TRMM3B42 was 0.2, 0.25, and 0.25° in longitude and latitude, respectively. TRMM-PR data were resampled from orbit-based TRMM 2A25 datasets. The near-surface rain rate from 2A25 was used. The units of all datasets were converted to mm day^{-1}. TRMM-PR, GSMaP-MWR, and TRMM3B42 datasets were used for over 10 years, from 1998 to 2007, nine years, from 1998 to 2006, and over 10 years, from 1998 to 2007, respectively. The GSMaP-MWR data were estimated from the passive microwave brightness temperature observed by several satellites. The TRMM3B42 data were based on infrared-radiation and passive microwave imagers and PR. To examine the rainfall-top height ("storm height"), the TRMM 2A23 dataset (Awaka et al., 1997) was used for over 10 years, from 1998 to 2007. Storm height was also resampled to 0.2° in longitude and latitude from the orbit-based 2A23 dataset. The storm height was calculated from the vertical profile of TRMM-PR, which is an advantage of the TRMM-PR dataset. For surface-rainfall data, the Global Precipitation Climatology Centre (GPCC, Schneider et al., 2008) Version 4 dataset was used. This was a gridded precipitation data on a 0.5×0.5 global grid over land from 1998 to 2007.

2.3. Atmospheric circulation

For this study, Japanese 25-year Reanalysis (JRA25, Onogi et al., 2007) and Japanese Meteorological Agency (JMA) Climate Data Assimilation System (JCDAS) datasets were used to examine climatological low-level wind fields and cold surges, including zonal and meridional winds (u,v). The datasets were global in coverage, with 2.5° spatial resolution and 6-hourly temporal resolution. In this study, the daily mean and monthly mean values of all atmospheric elements were calculated from the original data.

2.4. Cloud data procedure

To obtain albedos from the unphysical counted VIS values, the unphysical counted values were converted to physical albedos using the provided VIS calibration tables. In addition, the physical albedo values were revised as,

$$\alpha' = \alpha / \cos\theta_i, \tag{1}$$

where i is a grid, α is the unrevised VIS albedo value, α' is the revised albedo value divided by $\cos\theta_i$, and θ_i is the solar zenith angle. The threshold value of cloud existence from VIS was 0.40, as used in Kurosaki and Kimura (2002).

$$\text{cloud cover, when } \alpha' \geq 0.4 \tag{2}$$

$$\text{land}-\text{surface, when } \alpha' < 0.4. \tag{3}$$

Blackbody temperature T_{bb} values were converted from the unphysical counted values of IR1 using the calibration tables for IR1. To calculate the cloud-top temperatures, the cloud-cover area was first defined. Because the spatial resolutions of IR1 and VIS were different, this study tried to estimate the cloud-cover region using IR1. Fig. 2 is a

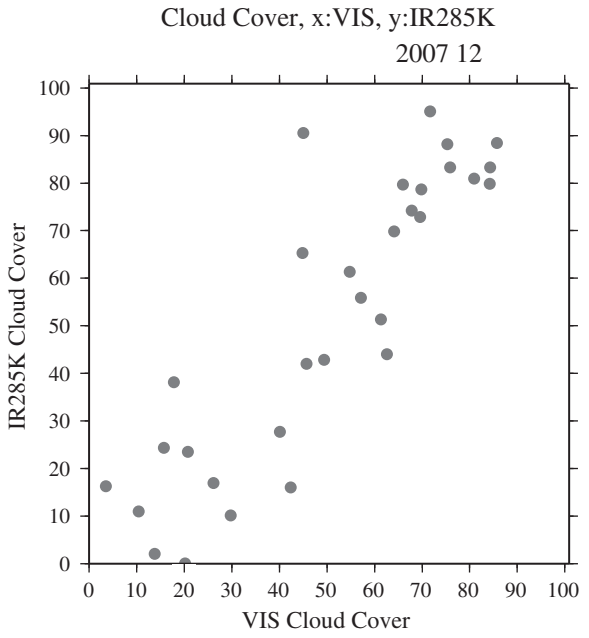

Fig. 2. Scatter plot of cloud covers determined by VIS (x-axis) and IR1 (y-axis) for December 2007 over the reference region (Fig. 1). Units are expressed as percentages.

comparison of the cloud coverage from VIS and IR1 over the reference region; as is evident, they were highly correlated. When the threshold value of T_{bb} (285 K) was used, the scatter plot between the cloud cover derived from the revised albedo observed by VIS and the estimated cloud cover derived from warmer than T_{bb} of 285 K observed from IR1 at 11:30 LST over the reference area for December 2007 basically showed close agreement (Fig. 2). The temperature 285 K (11.85 °C) was mostly lower than the surface skin temperature over the region, except for the mountainous region, as determined from an examination of the surface temperature of JRA25. Thus, the daily mean cloud-top temperature over the reference area was defined as

$$\Sigma\delta_i T_{bb}/\Sigma\delta_i \tag{4}$$

$$\delta_i = 1, \text{ when } T_{bb} \le 285 \text{ K}$$

$$\delta_i = 0, \text{ when } T_{bb} > 285 \text{ K}.$$

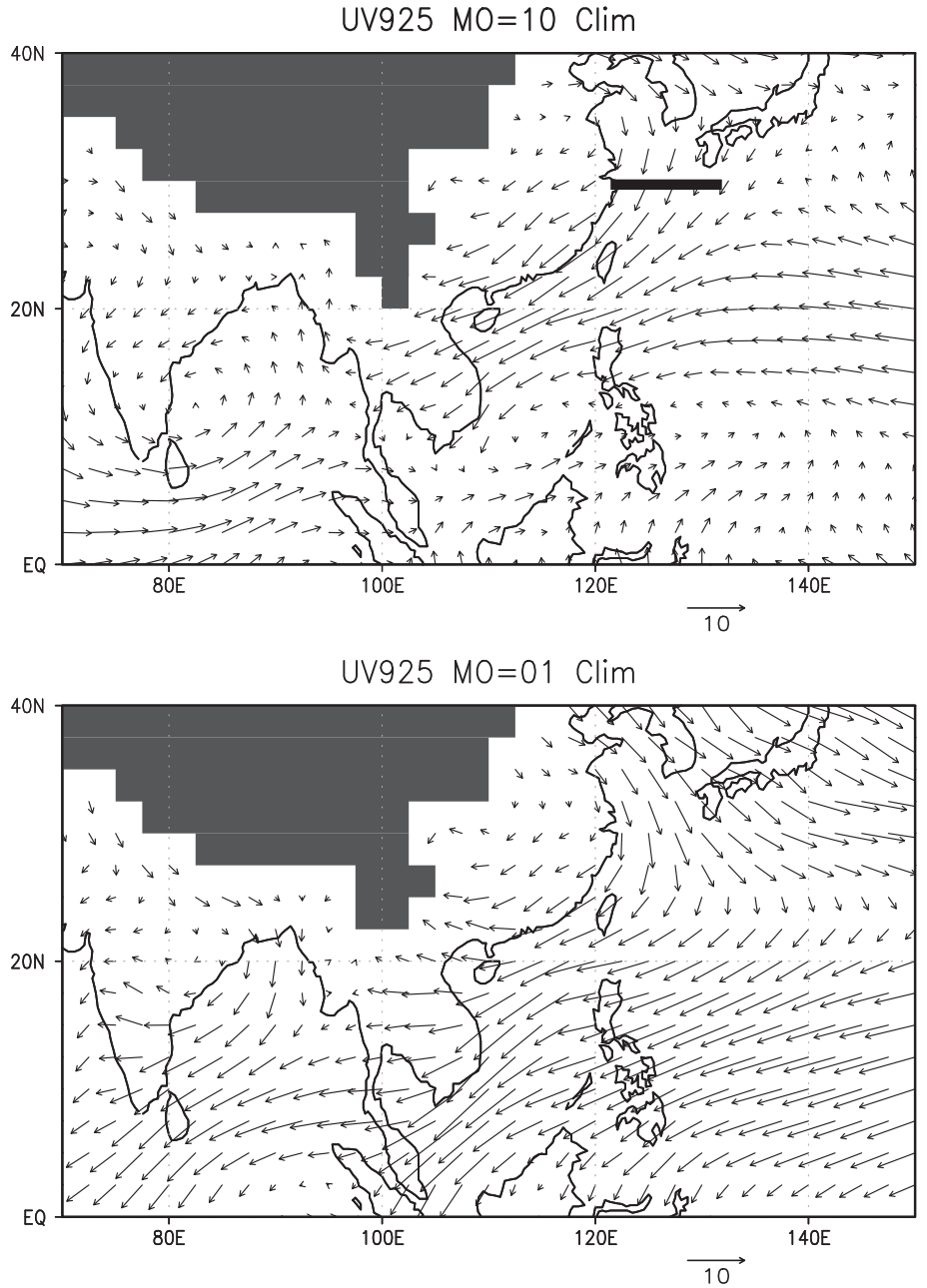

Fig. 3. Climatological 925-hPa winds in October (upper panel) and January (lower panel) averaged from 1979 to 2004. The black shades over land denote orographical masks at 925 hPa. Units are expressed as m s^{-1}. The horizontal black bar in the upper panel over the East China Sea denotes the averaged line of the cold surge index in Fig. 9.

Although the mean T_{bb} value over the cloud-cover area within the reference area may include surface temperature in mountainous regions, the effect is negligible. Thus, this study used the mean cloud-top temperature, T_{bb}, which was averaged over the cloud-covered region estimated from IR1. Although T_{bb} may also sometimes be affected by thin clouds in the upper troposphere, such as cirrus, an examination of many IR1 images confirmed that the effect was small, at least over the study area and during the study period.

2.5. Characteristics of rainfall datasets

This subsection introduces the different characteristics of rainfall datasets. The data quality of TRMM-PR was almost homogeneous over ocean and land. Thus, the spatial pattern of TRMM-PR rainfall is probably the most realistic among them. For example, Takahashi et al. (2010a) showed close agreement between the spatial patterns of TRMM-PR and rain-gauge rainfall in the summer monsoon rainfall, although the total rainfall amount of TRMM-PR was generally underestimated. The quality of GSMaP-MWR may be good over the open ocean. However, the estimation algorithm of GSMaP-MWR was different over land and ocean. Thus, GSMaP-MWR may have spatial gaps between ocean and land. In addition, TRMM3B42 has the advantage of higher temporal resolution. TRMM3B42 may be affected by non-precipitating clouds, such as anvil clouds, because it includes an IR-based estimation. TRMM-PR and GSMaP-MWR were not affected by the advected clouds without precipitation, which is an advantage. The characteristics among PR, microwave, and IR sensors were compared for the precipitation system over the tropics and mid-latitudes (Yamamoto et al., 2008). Moreover, GPCC was produced from rain-gauge observations, which pose the problem of generating a spatial representation from point observations.

3. Results

3.1. Climatological wind fields

In one previous study, it was noted that rainfall along the eastern coast of the Indochina Peninsula in northern fall and winter was associated with low-level winds (Chang et al., 2005b). To examine the relationship between low-level winds and cloud-precipitation activity, a climatological low-level wind pattern over the Southeast Asian regions is shown in Fig. 3. In northern fall and winter, northeasterly winds mostly prevailed over the eastern coast of the Indochina Peninsula. The monsoon northeasterlies in October and November were basically as strong as those in December, January, and February along the eastern coast of the northern Indochina Peninsula and weaker along the eastern coast of the southern Indochina Peninsula.

3.2. Cloud activity

To understand cloud activity and its seasonal changes over Southeast Asia, the occurrence frequency of clouds derived from VIS is shown in Fig. 4. A high occurrence frequency of clouds in October was observed along the mountain ranges over the whole Indochina Peninsula, and it corresponded to the tops of the mountain ranges (Fig. 4a). These clouds were likely to have developed due to thermally induced local circulations. The spatial distribution of cloud-occurrence frequency in October was similar to that in November (not shown). On the other hand, an extremely high frequency of clouds was observed in January only over the windward side of the mountain ranges, especially the eastern side of the Annum mountain range, over the Indochina Peninsula (Fig. 4b). These clouds over the windward side are likely to be formed by dynamically forced upward motions by the Indochina land-mass. In addition, a moderately high frequency was observed over the broad regions from the coast to inland China. Similar

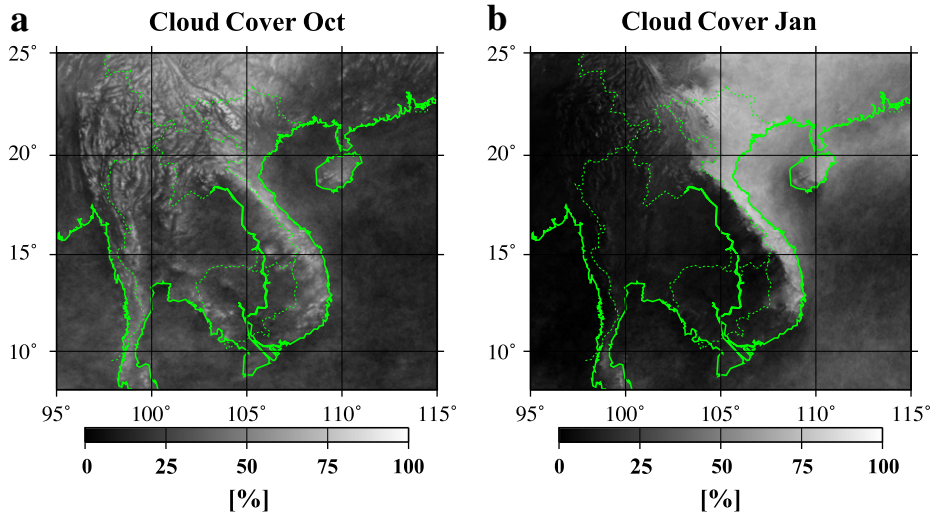

Fig. 4. Occurrence frequency of clouds in October (a) and in January (b). The existence of clouds was determined from VIS images. White (black) indicates more (less) frequent cloud activity.

distributions of cloud activity were noted in December and February (not shown). Compared with October and November (not shown), a higher cloud-occurrence frequency was observed in December, January, and February over the eastern coast of the Indochina Peninsula. This indicates that cloud occurrence in December, January, and February was more frequent or the cloud lifetimes were longer, although the monsoon northeasterly prevailed over the five months.

3.3. Seasonal march of rainfall

To understand the seasonal march of rainfall, various rainfall datasets were analyzed. Currently, rainfall amounts deviate among the datasets, which are usually used in climatological, meteorological, or related studies. More inter-comparisons are needed for precise rainfall estimation. Few inter-comparison studies of rainfall datasets over the Asian winter monsoon region in northern winter have been performed. The rainfall maps from four kinds of datasets for each month provide not only the climatological seasonal march of rainfall but also discrepancies in rainfall estimations from different observational methods.

In November, high rainfall amounts were observed over the coastal region in Vietnam (Fig. 5). The spatial pattern in November was similar to that in October (not shown). The spatial maximum of TRMM-PR rainfall corresponded to the maxima of GSMaP-MWR and TRMM3B42 rainfall.

In December, the total rainfall decreased more than that in November. High rainfall offshore of the eastern Indochina

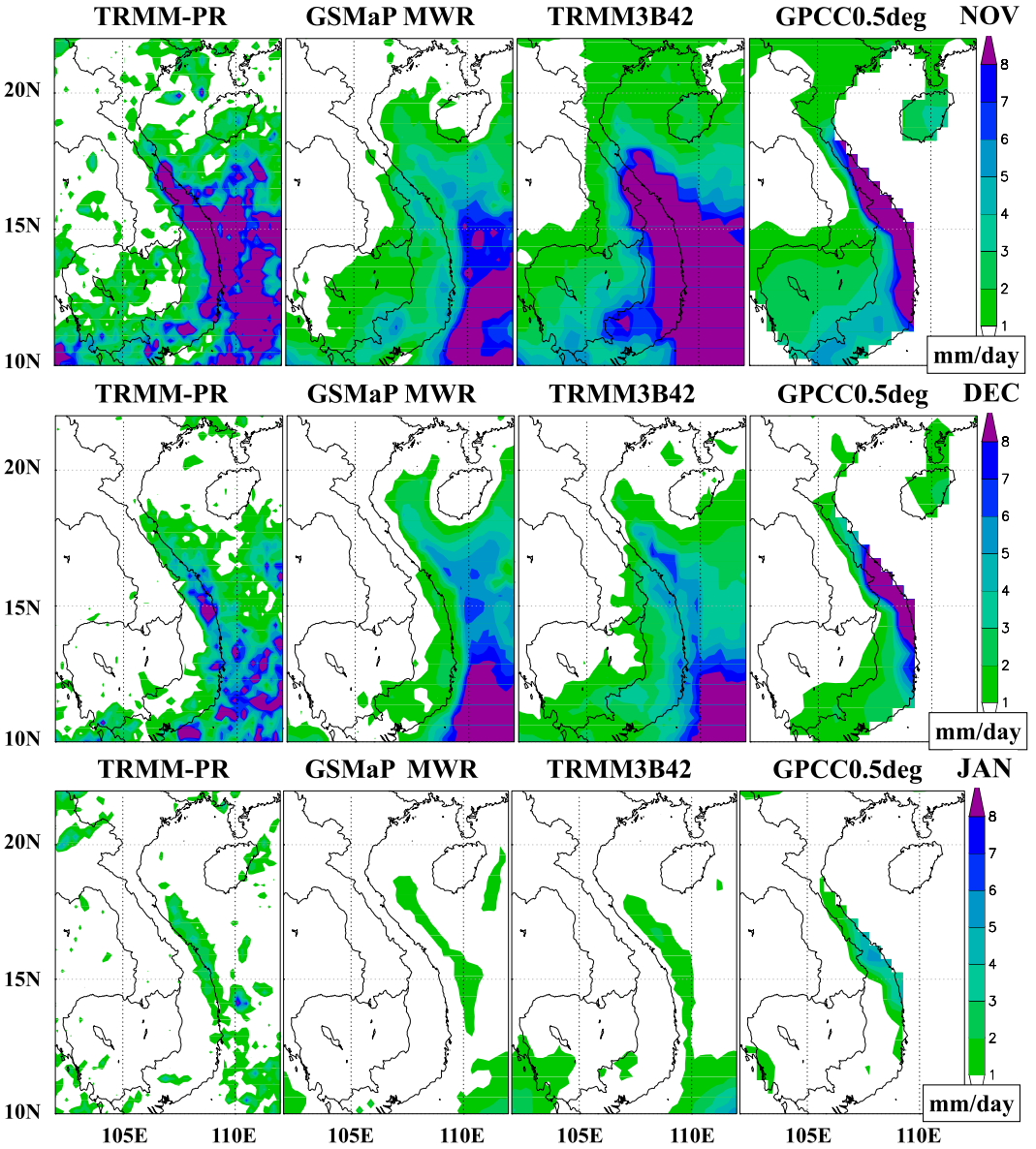

Fig. 5. Monthly rainfall amounts in four datasets (TRMM-PR, GSMaP-MWR, TRMM3B42, and GPCC) over the eastern Indochina Peninsula in November (upper panels), December (middle panels), and January (lower panels). Units are expressed as mm day^{-1}.

Peninsula was not found in TRMM-PR. The oceanic peak in GSMaP-MWR and TRMM3B42 was probably overestimated. The GSMaP-MWR rainfall amount over the ocean was higher for many months, which may have been due to the different algorithms used over land and ocean. The overestimation of TRMM3B42 can be partly explained by the effect of a microwave imager because TRMM3B42 used combined microwave- and IR-based estimations. A comparison of TRMM3B42 with T_{bb} observed by MTSAT-1 showed very similar patterns in space and time, which suggests that TRMM3B42 is also affected by the IR-based estimation. In addition, the spatial pattern of TRMM3B42 had an artificial gap between west and east of the 105°E meridional line over the Indochina Peninsula in November (little rainfall west of the 105°E latitudinal line) and between west and east of the 107°E meridional line over the Indochina Peninsula in December (little rainfall west of the 107°E latitudinal line). The other datasets showed that a horizontal gradient of rainfall amount is basically found along the mountain ranges and coastlines. However, the cause was not specified.

In January, the spatial map of TRMM-PR showed weak rainfall over coastal land and over ocean near the coast of central Vietnam (Fig. 5). The GPCC showed a spatial maximum in central Vietnam that was in good agreement with the TRMM-PR. The situation was very similar to that in December and February (not shown). The GSMaP-MWR and TRMM3B42 showed weak offshore rainfall in December and January without a weak peak over land, which was inconsistent with

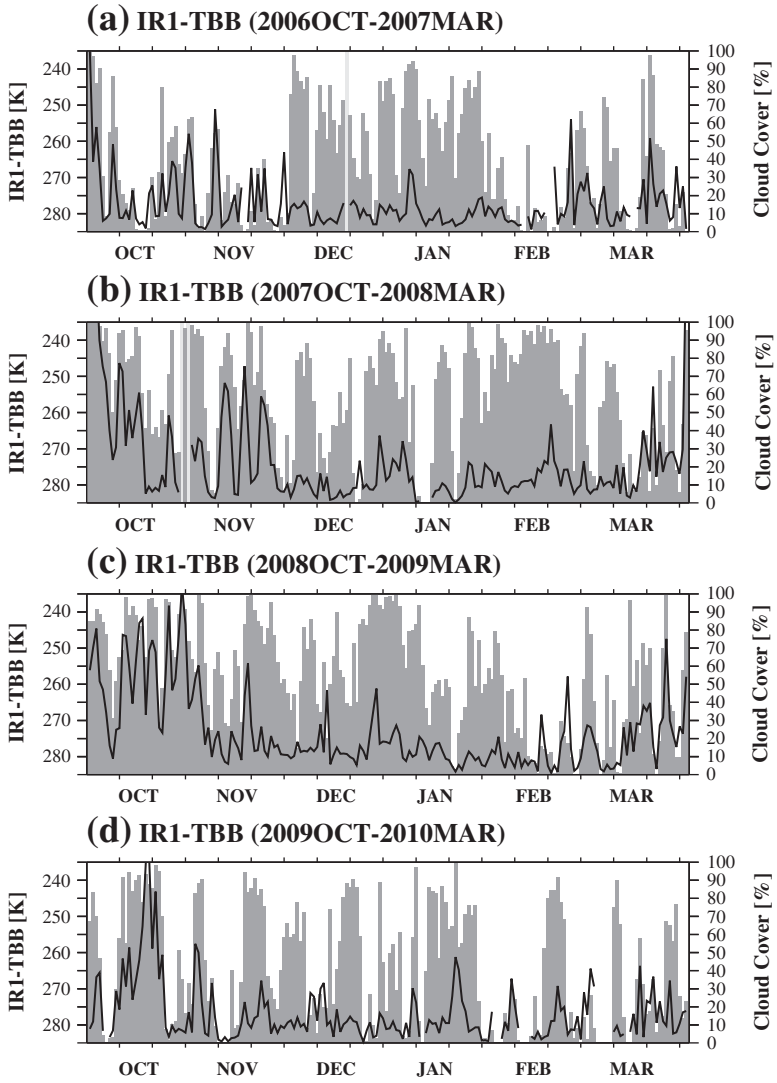

Fig. 6. Time series of cloud coverage (gray bar; right-hand side axis) over the eastern coast of the Indochina Peninsula (the reference region in Fig. 1) and averaged cloud-top temperature (solid line; left-hand side axis) for (a) 2006/2007, (b) 2007/2008, (c) 2008/2009, and (d) 2009/2010 northern winters. The averaged cloud-top temperature was omitted during periods of no cloud coverage or no observation. Light-gray bars show missing values. Cloud coverage was determined when T_{bb} was lower than 285 K at a grid point. Units are percent (vertical right-hand axis). The averaged cloud temperature was computed by averaging T_{bb} over the assumed cloud area (T_{bb}<285 K). Units are K (vertical left-hand axis). To facilitate an understanding of cloud-top height (cooler is higher), the axis of the T_{bb} (see left-hand y-axis) is reversed. The marks on the horizontal axis were plotted at 10-day intervals from 1 October.

the TRMM-PR. Again, the underestimation of GSMaP-MWR rainfall over the coastal region can be explained in the same way as that in other months. These results indicated that it is difficult to obtain an estimation with a microwave imager over the coastal region.

The spatial distribution of rainfall peaked along the eastern coast of the Indochina Peninsula, which can be associated with the low-level winter monsoon northeasterlies. The seasonal marches of precipitation observed by the four different datasets showed the similar tendency that a decrease in precipitation from northern fall to winter, although cloud activity and winter monsoon northeasterlies were still dominant over the region. In addition, the rainfall pattern was not exactly the same as the cloud-occurrence pattern, demonstrating that both cloud and rainfall analyses are necessary to obtain more detailed information of cloud and precipitation climatology. Obtaining rainfall estimations along the coastal regions remains complicated because of the microwave sensors used. IR data are not particularly accurate when used for spatially high-resolution estimations of precipitation. More inter-comparisons among rainfall products over various regions and seasons are required to improve the rainfall product in the future.

3.4. Cloud- and rainfall (storm)-top heights

This subsection investigates the characteristics and seasonal variation of clouds over the eastern coast of the Indochina Peninsula.

Fig. 6 shows a time-series of cloud coverage and cloud-top temperature at 11:30 LST over the eastern Indochina Peninsula. Cloud coverage varies on synoptic and intraseasonal time scales. The cloud-top temperature, which synchronizes with the cloud cover, also varies with the time scale. The mean cloud-top temperatures in October, November, and March were relatively lower than those in December, January, and February, indicating that taller clouds developed in October, November, and March than those in the northern winter months. Taking the surface temperature T_S and temperature lapse rate to be 290 K and 6.5 K km^{-1}, respectively, a rough estimation formula for the cloud-top height as a function of the cloud-top temperature may be written as follows, $\Delta Z = (T_S - T_{CTOP})/6.5$. Here, ΔZ km is altitude, when we take the bottom height as 0 km, T_S is the air temperature at the surface, and T_{CTOP} is the cloud-top temperature observed by satellite, i.e., T_{bb}. Below the cloud layer, the dry adiabatic lapse rate is 9.8 K km^{-1}, and within the cloud, a moist adiabatic lapse rate of approximately 6 K km^{-1} prevails. However, the height of the cloud base cannot be obtained from satellite observations. A cloud-top temperature of 260 K occurs at about 4.5-km altitude in November, and one of 275 K occurs at about 2.5-km altitude in January. In addition, the changes in cloud-top temperature may be consistent with seasonal changes in the temperature inversion layer over the Indochina Peninsula (Nodzu et al., 2006). Thus, low clouds occurred in December, January, and February, whereas relatively deeper clouds developed in October and March. November may be considered a transition period from deeper clouds to shallower clouds.

In addition, the diurnal variation in cloud-top temperature was examined to understand the diurnally developing features of clouds in the region. The occurrence frequency of T_{bb} as a function of time over the reference area was calculated (Fig. 7). Diurnal variation in cloud-top temperature over the reference area was predominant in October (Fig. 7) and November (not shown) but unclear in December (not shown), January (Fig. 7), and February (not shown). In October and November, lower T_{bb} values were frequently observed around 13:30 LST to 16:30 LST over the region. This indicates that clouds were well developed in the early afternoon in October and November. Daytime-developing clouds are probably associated with thermally induced local circulations. This characteristic of diurnally developing clouds is consistent with the spatial distribution of cloud-occurrence frequency (Fig. 4). T_{bb} around 280 K (about 7 °C) was frequently observed throughout the day in January. This probably indicates that diurnal cloud variations were not prominent, which is consistent with orographically induced clouds associated with the winter monsoon northeasterly. Hence, well-developed convective clouds probably occurred in October and November, whereas

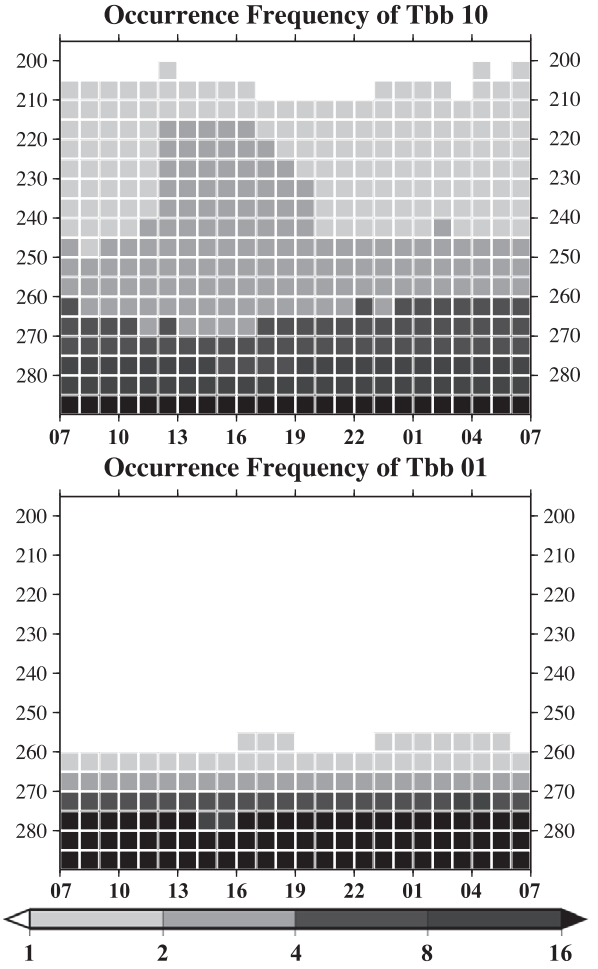

Fig. 7. Diurnal variation in the frequency of T_{bb} over the eastern coast of the Indochina Peninsula in October (upper panel) and in January (lower panel). Higher values than 290 K were omitted. Units are expressed in percent. To facilitate an understanding of cloud-top height (cooler is higher), the axis of the T_{bb} (see vertical axis) is reversed.

low-cloud cover occurred throughout the day in December, January, and February.

Additionally, the storm height (rainfall-top height) can be observed by TRMM-PR (Fig. 8). Interestingly, the storm height during rainfall showed very clear seasonal changes (Fig. 8). In October, the storm height was about 5.5 km along the eastern coast of the Indochina Peninsula. In November, the storm height was approximately 4 km along the eastern coast of the Indochina Peninsula (not shown). In December and January, the storm heights were 2 to 3 km over the eastern Indochina Peninsula, although the storm height in December was relatively higher than that in January. Storm height above 8 km was observed over the inland of the Indochina Peninsula in January, which can be understood as well-developed convective systems, although the occurrence frequency was very low. In this manner, the storm height over the region gradually decreased from northern fall to winter. The changes in storm heights within the Asian winter monsoon period were very similar to those in cloud-top temperature. Thus, cloud- and rainfall-top heights decreased within the same winter monsoon spell when the monsoon northeasterly prevailed. In other words, the cloud-precipitation characteristics changed during the winter monsoon spell.

4. Discussion

4.1. Impact of cold surges on cloud activity

As shown in the previous section, the clouds varied on synoptic and intraseasonal time scales. The time scales of cloud variability corresponded to that of the cold surges in the Asian winter monsoon (Compo et al., 1999). Concurrent with the cold surges of the Asian winter monsoon, it is quite possible that cloud activity would be associated with the mid-latitude cold surges. To understand the synoptic and intraseasonal variations in cloud activity over Southeast Asia associated with the cold surges of the Asian winter monsoon, a time series of cloud coverage and a cold surge index over the East China Sea were shown in Fig. 9. The index of cold surges is based on a 3–61-day bandpass-filtered 925-hPa meridional wind over 120°E–130°E along 30°N (shown in Fig. 3). To extract the synoptic and intraseasonal components, a simple 3–61-day bandpass filter was applied to the cold surge index. Specifically, a seasonal component (61-day running mean) was subtracted from the 3-day running mean time series of the 925-hPa meridional wind.

Cloud coverage drastically increases over the region, soon after the occurrence of cold surges over the East China Sea (Fig. 9). For example, from late December 2006 to mid-January 2007, three clear cold surges occurred, which likely resulted in high cloud cover immediately after their occurrence. In addition, the same tendency was clear in December 2007 and January 2008. Moreover, in the other years, a similar lag-relationship, although with varying time-scales of the cold surges, was evident. The lag-relationship clearly showed the association between cloud formation over the eastern coast of the Indochina Peninsula and cold surges of the Asian winter monsoon. However, the timing of the disappearance of clouds was later than the weakening of the cold surges, which probably indicates that cold surges formed low-level clouds along the eastern coast of the Indochina Peninsula and the clouds remained from a few to several days after the cold surge events. Thus, the development of low clouds along the eastern coast of the Indochina Peninsula was observed with the mid-latitude cold surges. After the formation of the clouds, low clouds may remain during the weakening phase of the cold surges.

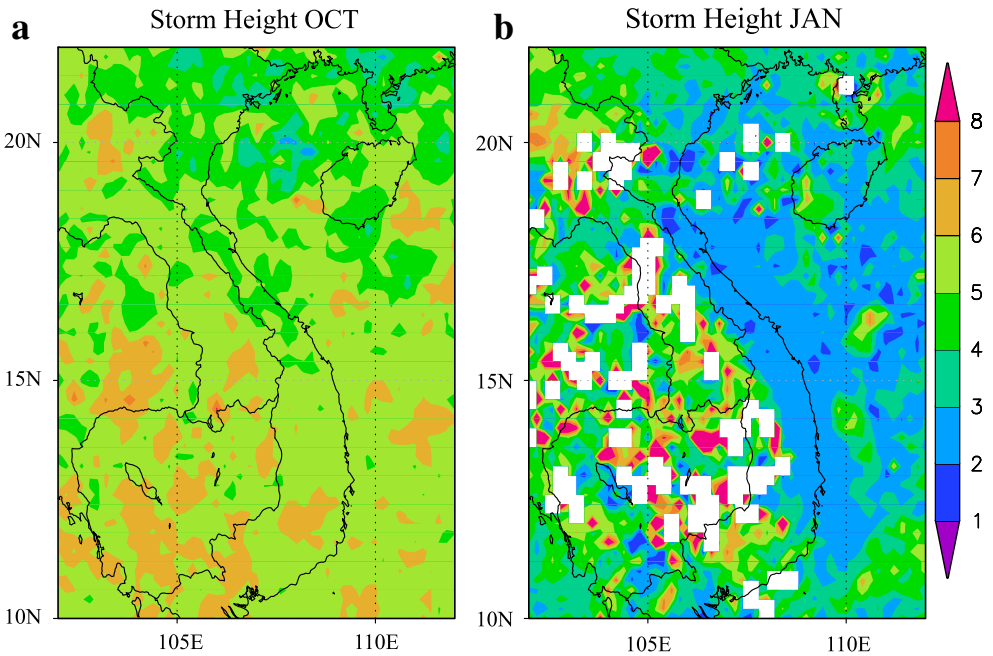

Fig. 8. Monthly mean storm height (rainfall-top height) observed by TRMM-PR (2A23 product) in October (a) and January (b). All observations with rainfall were averaged for 10 years. Units are expressed in kilometers. The unshaded areas denote no precipitation.

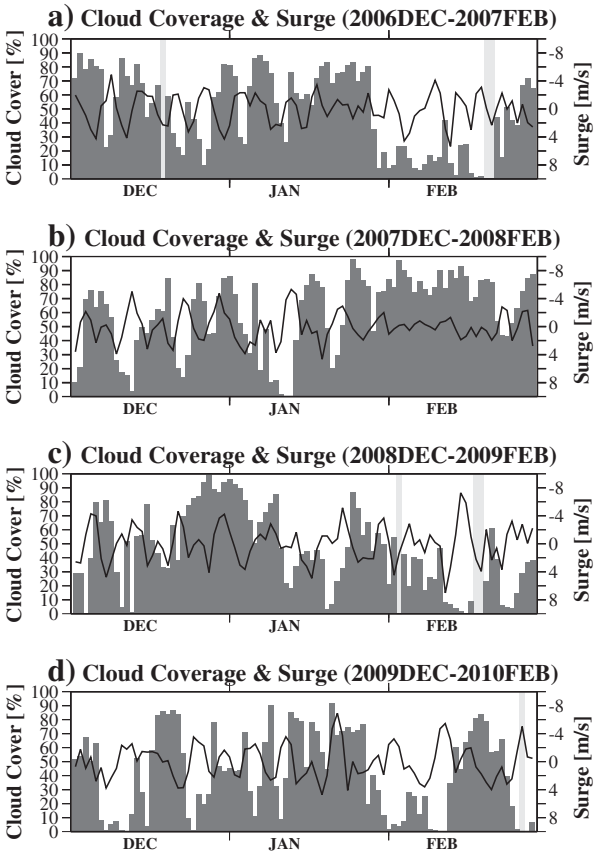

Fig. 9. Time series of cloud coverage (gray bar) over the eastern coast of the Indochina Peninsula (the reference region in Fig. 1) and a cold surge index over the East China Sea (solid line; shown in Fig. 3) for (a) 2006/2007, (b) 2007/2008, (c) 2008/2009, and (d) 2009/2010 northern winters. Light-gray bars show that MTSAT-1 values were missing. A 3–61-day bandpass filter was applied to the surge index. The unit of cloud coverage is a percentage, as indicated by the left-hand y-axis. The unit of winds is m s^{-1}. To facilitate comparison of the cloud coverage with the surge index, the axis of the surge index (see right-hand y-axis) is reversed.

To investigate the impact of mid-latitude cold surges on the cloud activity during December, January, and February over the eastern Indochina Peninsula, a lag-composite analysis of cloud cover was conducted (Fig. 10), using the bandpass-filtered meridional wind over the East China Sea. The threshold value was determined as $\pm 1.5\ \sigma$ from the mean, where σ is the daily standard deviation of the 925-hPa meridional wind from December to February at the reference point over four northern winters from 2006/07 to 2009/10. The peaks of the filtered meridional wind were determined as Lag 0 day, which will be referred to as Lag 0 day. To avoid duplication of the same events, one event per week was chosen. Over 4 years, 17 events were chosen.

Less frequent cloud cover was found on Lag −2 day over the Indochina Peninsula and southern China compared with the monthly mean occurrence frequency of clouds (Fig. 10). On Lag 0 day, less frequent cloud activity occurred. By Lag 2 day, the cloud activity had become frequent, which indicates that the cold surges developed clouds over these regions. Furthermore, cloud activity over southern China had disappeared by Lag 4 day. A high frequency of cloud occurrence was also found over the eastern Indochina Peninsula on Lag 4 day, suggesting that the clouds were still there in the weakening phase of the mid-latitude cold surges. The result of the lag-composite analysis clearly showed that cloud activity over the eastern Indochina Peninsula and southern China in northern winter was strongly associated with the mid-latitude cold surges. Therefore, the low clouds along the eastern coast of the Indochina Peninsula were not only affected by the mean northeasterly but also modulated by the cold surges of the Asian winter monsoon.

4.2. Seasonal changes in the cloud-precipitation system

The previous section examined the low clouds without significant rainfall prevailed in December, January, and February. The spatial distribution of clouds and cloud-top temperature and its diurnal cycle was consistent with the formation mechanism of low clouds associated with the orographically forced upward motions. However, cloud-precipitation systems with relatively higher clouds with a diurnal cycle occurred over the eastern Indochina Peninsula in October and November. The mechanism behind the developed cloud-precipitation systems in October and November is still unclear. Thus, this subsection discusses the characteristics of cloud and precipitation systems in northern fall.

Takahashi and Yasunari (2006, 2008); Takahashi et al. (2009), and Nguyen-Thi et al. (2012) showed that tropical

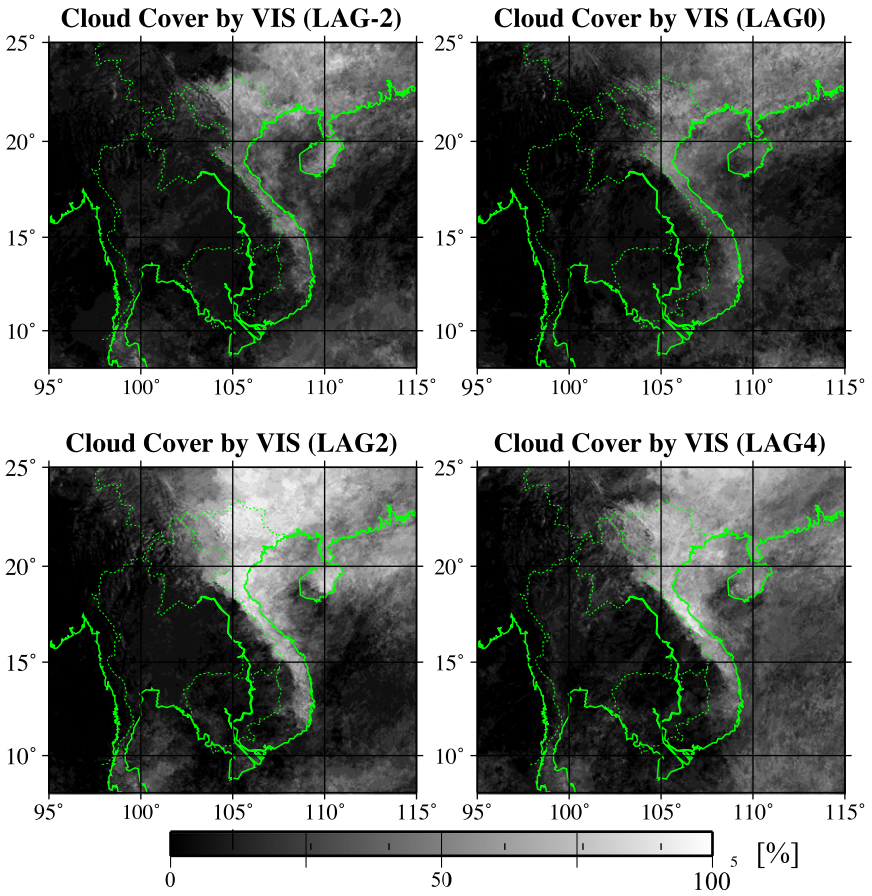

Fig. 10. Lag-composite analysis of cloud occurrence frequency during December, January, and February based on mid-latitude cold surges on Lag −2 day, Lag 0 day, Lag 2 day and Lag 4 day.

cyclone activity is enhanced over the South China Sea and the Philippine Sea during northern fall. Yokoi et al. (2007) showed that westward-propagating disturbances, including tropical cyclones, are dominant over the eastern Indochina Peninsula from August to November. In addition, Yokoi and Matsumoto (2008) noted that heavy rainfall events over the Indochina Peninsula were associated with tropical cyclone activity over the South China Sea in early November. Recently, Takahashi (2011) suggested that a major contributor to long-term changes in rainfall over Southeast Asia, including this region, in September, October, and November is the long-term changes in tropical cyclone activity over the Bay of Bengal, the South China Sea, and the Philippine Sea. These results support the idea that the dominant cloud-precipitation system over the eastern Indochina Peninsula in northern fall is responsible for tropical cyclone activity. Moreover, Takahashi et al. (2010b) found that the diurnal precipitation variation is prominent in September even during the tropical cyclone spells. This is consistent with the developed cloud activity with diurnal variation, which was described in Section 3 of this study. Hence, this observational evidence is consistent with the well-developed cloud-precipitation systems associated with tropical cyclone activity, which vary diurnally. Furthermore, small rainfall amounts in December, January, and February are partly explained by the inactive tropical cyclone spells over and around the region.

5. Conclusions

This study investigated cloud and rainfall climatology over Southeast Asia in the northeast monsoon period using cloud and rainfall data derived mainly from satellite observations.

The results showed that the cloud and precipitation system changed within a winter monsoon period. High rainfall was observed during October and November, whereas little rainfall was observed during December, January, and February, although northeasterly winds of the Asian winter monsoon similarly prevailed in both the northern fall and winter. In October and November, well-developed cloud-precipitation systems occurred, with diurnal variation in cloud activity, while low clouds without significant rainfall cover throughout the day in December, January, and February. In addition, the cloud-precipitation system in the first half of the winter monsoon period is probably associated with tropical cyclone activity, although diurnal variation in cloud activity is still active. On the other hand, orographically forced upward motions associated with the monsoon northeasterlies form low clouds along the eastern coast of the Indochina Peninsula

during the latter half of the winter monsoon. This study clarified the sub-seasonal march of clouds and rainfall over the Asian winter monsoon region. Moreover, the low clouds occurred repeatedly and were associated with mid-latitude cold surges on synoptic and intraseasonal time scales.

Low clouds with little rainfall during northern winter may be associated with air quality over the eastern Indochina Peninsula. This would be an interesting subject for further study.

Acknowledgment

The author would like to acknowledge two anonymous reviewers for their helpful suggestions and comments. This work was partly supported by the "Green Network of Excellence (GRENE)" program by the Ministry of Education, Culture, Sports, Science, and Technology (MEXT), Japan, the Global Environment Research Fund (RFa-1101) of the Ministry of the Environment, Japan, the Leading Scientist Award Fund of Tokyo Metropolitan University, the 6th JAXA PMM Project No. 306, and a joint research program of the Center for Environmental Remote Sensing (CEReS), Chiba University.

References

Awaka, J., Iguchi, T., Kumagai, H., Okamoto, K., 1997. Rain type classification algorithm for TRMM precipitation radar. Geoscience and Remote Sensing, 1997. IGARSS'97. Remote Sensing—A Scientific Vision for Sustainable Development., 1997 IEEE International. IEEE, pp. 1633–1635.

Bony, S., Collins, W., Fillmore, D., 2000. Indian Ocean low clouds during the winter monsoon. J. Clim. 13, 2028–2043.

Chang, C., Liu, C., Kuo, H., 2003. Typhoon Vamei: an equatorial tropical cyclone formation. Geophys. Res. Lett. 30, 1150.

Chang, C., Harr, P., Chen, H., 2005a. Synoptic disturbances over the equatorial South China Sea and western Maritime Continent during boreal winter. Mon. Weather Rev. 133, 489–503.

Chang, C., Wang, Z., McBride, J., Liu, C., 2005b. Annual cycle of Southeast Asia–Maritime Continent rainfall and the asymmetric monsoon transition. J. Clim. 18, 287–301.

Compo, G., Kiladis, G., Webster, P., 1999. The horizontal and vertical structure of east Asian winter monsoon pressure surges. Q. J. R. Meteorol. Soc. 125, 29–54.

Goldenberg, S., Houze Jr., R., Churchill, D., 1990. Convective and stratiform components of a winter monsoon cloud cluster determined from geosynchronous infrared satellite data. J. Meteorol. Soc. Jpn. 68, 37–62.

Houze, R., Geotis, S., Marks Jr., F., West, A., 1981. Winter monsoon convection in the vicinity of North Borneo. Part I: structure and time variation of the clouds and precipitation. Mon. Weather Rev. 109, 1595–1614.

Huffman, G., Bolvin, D., Nelkin, E., Wolff, D., Adler, R., Gu, G., Hong, Y., Bowman, K., Stocker, E., 2007. The TRMM multisatellite precipitation analysis (TMPA): quasi-global, multiyear, combined-sensor precipitation estimates at fine scales. J. Hydrometeorol. 8, 38–55.

Ichikawa, H., Yasunari, T., 2006. Time-space characteristics of diurnal rainfall over Borneo and surrounding oceans as observed by TRMM–PR. J. Clim. 19, 1238–1260.

Iguchi, T., Kozu, T., Meneghini, R., Awaka, J., Okamoto, K., 2000. Rain-profiling algorithm for the TRMM precipitation radar. J. Appl. Meteorol. 39, 2038–2052.

Klein, S., Hartmann, D., 1993. The seasonal cycle of low stratiform clouds. J. Clim. 6, 1587–1606.

Kubota, T., Shige, S., Hashizume, H., Aonashi, K., Takahashi, N., Seto, S., Takayabu, Y., Ushio, T., Nakagawa, K., Iwanami, K., Kachi, M., Okamoto, K., 2007. Global precipitation map using satellite-borne microwave radiometers by the GSMaP project: production and validation. IEEE Trans. Geosci. Remote. Sens. 45, 2259–2275.

Kurosaki, Y., Kimura, F., 2002. Relationship between topography and daytime cloud activity around Tibetan Plateau. J. Meteorol. Soc. Jpn. 80, 1339–1355.

Nguyen-Thi, H.A., Matsumoto, J., Ngo-Duc, T., Endo, N., 2012. A climatological study of tropical cyclone rainfall in Vietnam. SOLA 8, 41–44.

Nodzu, M., Ogino, S., Tachibana, Y., Yamanaka, M., 2006. Climatological description of seasonal variations in lower-tropospheric temperature inversion layers over the Indochina Peninsula. J. Clim. 19, 3307–3319.

Onogi, K., Tsutsui, J., Koide, H., Sakamoto, M., Kobayashi, S., Hatsushika, H., Matsumoto, T., Yamazaki, N., Kamahori, H., Takahashi, K., Kadokura, S., Wada, K., Kato, K., Oyama, R., Ose, T., Mannoji, N., Taira, R., 2007. The JRA-25 reanalysis. J. Meteorol. Soc. Jpn. 85, 369–432.

Schneider, U., Fuchs, T., Meyer-Christoffer, A., Rudolf, B., 2008. Global Precipitation Analysis Products of the GPCC. Deutscher Wetterdienst. 12 pp. [Available online at http://www.gpcc.dwd.de.].

Takahashi, H.G., 2011. Long-term changes in rainfall and tropical cyclone activity over South and Southeast Asia. Adv. Geosci. 30, 17–22.

Takahashi, H.G., Yasunari, T., 2006. A climatological monsoon break in rainfall over Indochina—a singularity in the seasonal march of the Asian summer monsoon. J. Clim. 19, 1545–1556.

Takahashi, H.G., Yasunari, T., 2008. Decreasing trend in rainfall over Indochina during the late summer monsoon: impact of tropical cyclones. J. Meteorol. Soc. Jpn. 86, 429–438.

Takahashi, H.G., Yoshikane, T., Hara, M., Yasunari, T., 2009. High-resolution regional climate simulations of the long-term decrease in September rainfall over Indochina. Atmos. Sci. Lett. 10, 14–18.

Takahashi, H.G., Fujinami, H., Yasunari, T., Matsumoto, J., 2010a. Diurnal rainfall pattern observed by Tropical Rainfall Measuring Mission Precipitation Radar (TRMM-PR) around the Indochina Peninsula. J. Geophys. Res. 115, D07109.

Takahashi, H.G., Yoshikane, T., Hara, M., Takata, K., Yasunari, T., 2010b. High-resolution modelling of the potential impact of land surface conditions on regional climate over Indochina associated with the diurnal precipitation cycle. Int. J. Climatol. 30, 2004–2020.

Takahashi, H.G., Fukutomi, Y., Matsumoto, J., 2011. The impact of long-lasting northerly surges of the East Asian Winter monsoon on tropical cyclogenesis and its seasonal march. J. Meteorol. Soc. Jpn. 89A, 181–200.

Yamamoto, M., Furuzawa, F., Higuchi, A., Nakamura, K., 2008. Comparison of diurnal variations in precipitation systems observed by TRMM PR, TMI, and VIRS. J. Clim. 21, 4011–4028.

Yokoi, S., Matsumoto, J., 2008. Collaborative effects of cold surge and tropical depression-type disturbance on heavy rainfall in Central Vietnam. Mon. Weather Rev. 136, 3275–3287.

Yokoi, S., Satomura, T., Matsumoto, J., 2007. Climatological characteristics of the intraseasonal variation of precipitation over the Indochina Peninsula. J. Clim. 20, 5301–5315.